



UNIVERSITY OF LEEDS

This is a repository copy of *Polymer Hydrogels for Glutathione-Mediated Protein Release*.

White Rose Research Online URL for this paper:

<https://eprints.whiterose.ac.uk/105113/>

Version: Accepted Version

Article:

McAvan, BS, Khuphe, M orcid.org/0000-0002-6289-8675 and Thornton, PD orcid.org/0000-0003-3876-1617 (2017) Polymer Hydrogels for Glutathione-Mediated Protein Release. *European Polymer Journal*, 87. pp. 468-477. ISSN 0014-3057

<https://doi.org/10.1016/j.eurpolymj.2016.09.032>

© 2016. This manuscript version is made available under the CC-BY-NC-ND 4.0 license <http://creativecommons.org/licenses/by-nc-nd/4.0/>

Reuse

Items deposited in White Rose Research Online are protected by copyright, with all rights reserved unless indicated otherwise. They may be downloaded and/or printed for private study, or other acts as permitted by national copyright laws. The publisher or other rights holders may allow further reproduction and re-use of the full text version. This is indicated by the licence information on the White Rose Research Online record for the item.

Takedown

If you consider content in White Rose Research Online to be in breach of UK law, please notify us by emailing eprints@whiterose.ac.uk including the URL of the record and the reason for the withdrawal request.



eprints@whiterose.ac.uk
<https://eprints.whiterose.ac.uk/>

Polymer Hydrogels for Glutathione-Mediated Protein Release

Bethan S. McAvan*, Mthulisi Khuphe* and Paul D. Thornton[†]

School of Chemistry, University of Leeds, LS2 9JT, Leeds, United Kingdom

[†] Email: p.d.thornton@leeds.ac.uk

* These authors contributed equally to the research.

Abstract

The use of amine-terminated poly(ethylene glycol) star polymers as macroinitiators for the N-carboxyanhydride ring-opening polymerisation of *S-tert*-butylmercapto-L-cysteine N-carboxyanhydride is described to yield amphiphilic copolymers that are capable of forming discrete particles in aqueous solution. Poly(amino acid) deprotection liberates the pendant thiol groups that can then form covalent disulfide crosslinks with adjacent thiol groups and yield a crosslinked polymer that is capable of hydrogel formation. The model protein albumin–fluorescein isothiocyanate conjugate was encapsulated within the hydrogels produced, prior to its release upon hydrogel interaction with the reducing agent glutathione. Consequently, the stimuli-responsive polymers formed hold great promise as biomaterials capable of releasing a protein molecular cargo upon interaction with glutathione.

Keywords: Stimuli-responsive polymers; Glutathione-mediated degradation; Protein delivery; Polymeric biomaterials.

Introduction

Stimuli-responsive polymers are an important class of material that may readily be applied for the production of advanced biomaterials [1-3]. The controlled release of payload molecules from a polymeric carrier upon external stimulation enables the delivery of therapeutic agents

on-demand, as part of a highly-effective drug delivery system [4,5]. In addition, stimuli-responsive polymers may be utilised as scaffolds for tissue regeneration [6-8]. Consequently, polymers that are susceptible to a controlled response and/or degradation upon interaction with stimuli including alterations in environmental temperature [9], pH [10-12], and the presence of particular enzymes, are highly sought [13].

Polymers that undergo physical/chemical alterations upon interaction with reducing agents are also of significance for use within a biomedical context [14-16]. Glutathione (GSH) is a natural tripeptide that is abundant in the majority of animal cells. The thiol group of the cysteine unit of glutathione dictates that glutathione is a reducing agent; for instance the disulfide bonds that are formed within cytoplasmic proteins are reduced to cysteine units due to glutathione being an electron donor [17]. Micromolar concentrations of GSH are found within the blood plasma, compared to intracellular GSH concentrations of between 0.5 mM and 10 mM. This renders glutathione to be a particularly valid target for therapeutic treatment as extracellular drug release is minimised [18].

Employing a polymeric hydrogel as a carrier vehicle permits the controlled delivery of biomolecules, such as the protein drugs Trastuzumab, Bevacizumab and Rituximab, *in vivo* [19]. Polymer hydrogels are well-suited to the controlled delivery of proteins as they present an aqueous environment that prevents protein denaturation. The hydrogel enables the efficient encapsulation of the protein cargo, restricting its metabolisation whilst maintaining its bioactivity, and enables protein release at a pre-programmed rate upon stimulation. Such materials have been utilised for the delivery of growth factors as part of tissue regeneration, and the controlled delivery of proteins that act as therapeutic agents [20,21]. The relative ease of polymer hydrogel synthesis, coupled with the feasibility of creating materials that possess general biocompatibility, adds to their suitability for employment as drug delivery vehicles and scaffolds to promote tissue regeneration.

Hereon in we report the generation of poly(ethylene glycol) (PEG) star polymers that are terminated with cysteine oligomers for use as protein delivery vehicles. Cysteine is a particularly useful component of functional materials due to its pendant thiol group that may be utilised for thiol-ene 'click' reactions [22], or participate in the formation of disulfide bridges [23]. The terminal cysteine units were grafted by N-carboxyanhydride ring-opening polymerisation (NCA ROP) and possessed tertiary butyl protecting units to protect the thiol groups of the cysteine repeat units, thus producing an amphiphilic structure that possessed the capability to form discrete particles in aqueous solution. Cysteine deprotection liberated the thiol groups, enabling the polymers to undergo chemical crosslinking, *via* the formation of disulfide bridges, to yield a polymeric network. This polymeric network was able to uptake appreciable amounts of water, due to the considerable PEG content, and form hydrogels that were susceptible to reduction upon incubation with glutathione. The polymer hydrogels formed were able to encapsulate and selectively release the fluorescently labelled model protein bovine serum albumin, deeming them highly-applicable for the controlled release of protein payloads within reductive environments. It is envisaged that the hydrogels formed may act as scaffolds for tissue engineering that permit the release of a protein growth factors, and/or as protein delivery vehicles that perform payload release upon interaction with a reducing agent that is either present, or injected to the intended site of action, in both instances.

Materials and General Methods

Triphosgene ($\geq 98\%$), anhydrous ethyl acetate ($\geq 99.8\%$), n-hexane ($\geq 98\%$), anhydrous dimethylformamide (DMF) ($\geq 99.8\%$), diethyl ether ($\geq 99.8\%$), 4-arm amine-terminated poly(ethylene glycol) (PEG star polymer; 10,000 Da), cobalt phthalocyanine ($> 97\%$), *S-tert*-butylmercapto-L-cysteine, 1,4 Dithiothreitol ($\geq 97\%$), albumin–fluorescein isothiocyanate conjugate (FITC-albumin) and L-glutathione ($\geq 99.8\%$) were all acquired from Sigma Aldrich. α -Pinene ($\geq 98\%$) and phosphate buffered saline (PBS) tablets (Dulbecco 'A' tablets) were

supplied by Thermo Fisher Scientific Laboratories. HPLC grade water (18.2 M Ω .cm) was supplied by VWR International. All chemicals were used as received unless stated otherwise.

^1H NMR and ^{13}C NMR spectra were recorded at 25 °C on a Bruker Avance 500 MHz spectrometer and analysed using MestreNova® Research Lab software. Elemental analyses were conducted using a Thermo FlashEA Analyzer 1112 Series instrument. Fourier Transform-Infrared Spectroscopy (FTIR) measurements were performed on a Bruckner Alpha-P spectrometer, equipped with a diamond ATR crystal and the data was processed using Opus 7.2 software. Scanning electron microscopy (SEM) studies were performed on a JEOL JSM-6610LV microscope (Oxford Instruments) equipped with a field emission electron gun as an electron source, using a working distance of 11 mm. The accelerating voltage was varied between 5 kV and 15 kV. Fluorescence imaging was carried out using an Axio observer Z1 microscope (Zeiss Instruments) equipped with an AxioCam IC camera and an LD A-plan 5x0.15 Ph1 objective lens (excitation; 492 nm, emission; 515 nm, exposure time; 445 ms). Differential scanning calorimetry (DSC) analyses were carried out on a DSC Q20 unit (TA instruments) calibrated with indium and a nitrogen sample purge flow of 50 mL/min. A heating rate of 10 °C per minute was adopted for all samples. A TGA Auto Q20 unit (TA Instruments) was used to carry out thermogravimetric analysis (TGA). Samples were heated from room temperature at 10 °C per minute. A balance purge flow of 40 mL/minute and sample purge flow of 60 mL/minute were used. Dynamic light scattering (DLS) was conducted using a Malvern ZetaSizer NS. Sample equilibration was conducted for 1 minute prior to analysis.

Experimental Procedures

Synthesis of S-*tert*-Butylmercapto-L-Cysteine NCA

NCA synthesis was conducted using triphosgene for amino acid cyclisation [24]. S-*tert*-butylmercapto (STBM)-L-cysteine (5.00 g, 23.89 mmol) was dissolved in anhydrous ethyl acetate (60 mL) and injected under nitrogen flow into a three neck round bottom flask equipped

with a magnetic stirrer bar, condenser and dropping funnel. α -pinene (7.17 g, 52.62 mmol) was degassed and then injected into the reaction flask and the suspension was heated to reflux. Then, triphosgene (4.90 g, 16.5 mmol) dissolved in anhydrous ethyl acetate (20 mL) was added dropwise into the refluxing suspension over a period of 30 minutes. The reaction was then left to reflux for 4 hours, at which point all the suspension had dissolved. After cooling, the crude solution was concentrated by removing 75% of the ethyl acetate using rotary evaporation. The concentrated crude solution was precipitated from cold ethyl acetate/n-hexane (1:9 v/v) and left to stand at -18 °C for 24 hours. The precipitated product was isolated by gravitational filtration, purified further by repeated precipitation from ethyl acetate and n-hexane (1:9 v/v) and subsequently dried under vacuum to obtain the NCA as a white powder. Yield: 3.57 g, 15.17 mmol, 64%.

^1H NMR (500 MHz, CDCl_3 , δ , ppm): 6.37 (s, 1H, NH), 4.63 (dd, $J = 9.20, 2.9$ Hz, 1H, αCH), 2.99 (ddd, $J = 23.3, 14.0, 6.2$ Hz, 2H), 1.30 (s, 9H, *tert*-Butyl). FTIR: $\nu_{\text{max}}/\text{cm}^{-1}$ (solid): 3232 (NH), 2959 (CH), 1845 and 1805 (asymmetric anhydride C=O). ^{13}C NMR (125 MHz, CDCl_3 , δ , ppm):

Synthesis of Poly[(STBM-L-cysteine)_n]-*b*-(StarPEG_{10k})]

Macromolecules

A representative procedure for the syntheses of poly[(STBM-L-cysteine)_n]-*b*-(StarPEG_{10k})] macromolecules is given for a monomer:macroinitiator feed ratio of 10:1. STBM-L-cysteine NCA (0.19 g, 0.81 mmol) was dissolved in anhydrous DMF (20 mL) under nitrogen flow and then injected into a sealed Schlenk tube that was previously dried, evacuated, nitrogen-purged and equipped with a magnetic stirrer bar. Then, amine-terminated PEG star polymer (0.20 g, 0.02 mmol) was dissolved in anhydrous DMF (20 mL) and this solution was introduced under nitrogen flow to the NCA solution in the Schlenk tube. The reaction solution was then stirred under nitrogen flow for 96 hours at room temperature. The polymer obtained was subsequently precipitated out of solution by adding the reaction solution dropwise to an excess of cold

diethyl ether (1:10 v/v). The precipitate obtained was left to stand in the freezer (-18 °C) for 24 hours to enhance polymer precipitation. The polymer was eventually isolated by centrifugation (2000 rpm, 10 min, -5 °C) and dried *in vacuo* at 40 °C for 24 hours. The same procedure was followed for the synthesis of other poly(amino acid)-grafted macromolecules using monomer:macroinitiator feed ratios of 5:1 and 20:1.

¹H NMR (500 MHz, TFA, δ, ppm): 7.48 (s, NH), 5.53-4.75 (m, αCH), 4.25-3.76 (m, PEG), 2.45-2.34 (d, -S-S-CH₂), 1.73-1.38 (m, *tert*-Butyl). FTIR: $\nu_{\max}/\text{cm}^{-1}$ (solid): 3325 (NH), 2879 (CH), 1676 (C=O secondary amide).

Poly[(STBM-L-cysteine₁₀)₄-*b*-(StarPEG_{10k})] Deprotection

A representative procedure for the deprotection of the poly(amino acid)-grafted macromolecules is given using an outline for the deprotection of poly[(STBM-L-cysteine₁₀)₄-*b*-(StarPEG_{10k})]. Poly[(STBM-L-cysteine₁₀)₄-*b*-(StarPEG_{10k})] (0.21 g, 0.02 mmol) was dissolved in anhydrous DMF (20 mL) and injected into a Schlenk tube equipped with a magnetic stirrer bar. Dithiothreitol (DTT) (0.20 g, 1.3 mmol) was dissolved in anhydrous DMF (5 mL) and added to the polymer solution and the reaction was stirred at 60 °C for 120 hours. The reaction mixture was then dialysed against deionised water for 96 hours and the deprotected polymer was subsequently obtained *via* lyophilisation.

¹H NMR (500 MHz, DMSO, δ, ppm): 7.97 (s, NH), 5.23-5.22 (d, αCH), 3.52-3.33 (m, PEG), 2.77-2.51 (m, -S-S-CH₂). FTIR: $\nu_{\max}/\text{cm}^{-1}$ (solid): 3305 (NH), 2875 (CH), 1682 (C=O secondary amide).

Polymer Crosslinking

Poly[(L-cysteine₁₀)₄-*b*-(StarPEG_{10k})] (0.20 g, 0.02 mmol) was dissolved in anhydrous DMF and then injected into a Schlenk tube. Cobalt phthalocyanine (10 mg, 0.02 mmol) was dissolved in anhydrous DMF (5 mL) and added to the polymer solution. The reaction was stirred at room

temperature for 24 hours. The reaction mass was then added to an excess of cold diethyl ether (1:10 v/v) and left to stand at -18°C for 24 hours. The crosslinked material was isolated by centrifugation (2000 rpm, 20 min) and dried under vacuum at 30 °C for 48 hours. FTIR: $\nu_{\text{max}}/\text{cm}^{-1}$ (solid): 3270 (NH), 2864 (CH), 1667 (C=O secondary amide).

Nanoprecipitation and Dynamic Light Scattering

Polymer solutions (5 mg/mL) were obtained by dissolving Poly[(STBM-L-cysteine)_n]-*b*-(StarPEG_{10k}) macromolecules in DMF. Then, samples (40 μL) were aliquoted from the respective solutions and added dropwise to ultra-pure water (18.2 Megohms, 20 mL). The samples were allowed to stir for 30 minutes and the particle size and size distribution analysed by DLS.

Scanning Electron Microscopy

For the determination of particle size and morphology, a drop was obtained from each nanoprecipitated sample and deposited onto a microscope glass slide mounted onto an SEM stub. For the determination of the morphology of hydrogel scaffolds, xerogels were prepared by lyophilisation of the hydrogels for 48 hours. The xerogels obtained were then mounted onto SEM stubs using conductive tap and then sputter-coated with a thin layer of gold using a current of 20 mA for 2 minutes in a Quorum Q150RS sputter-coater.

Advanced Polymer Chromatography (APC)

The molecular weight distributions of the polymers formed were assessed by advanced polymer chromatography (APC), using DMF (1 g/L LiBr) as the eluent. Analyses were carried out using a Waters ACQUITY APC system equipped with an ACQUITY APC AQ (200 Å, 2.5 μm) column packed with bridged ethylene hybrid particles, using an ACQUITY refractive index

detector. The column temperature was maintained at 40 °C and the flow rate at 0.5 mL/minute. The data generated was processed using Empower 3 software.

Water Uptake Studies

Hydrogel scaffolds were allowed to dry in a vacuum oven (48 hours, 37 °C). The dry scaffolds (10 mg) were then soaked in excess deionised water and water uptake by the scaffolds was determined by monitoring the weight of the scaffolds until a point of saturation was reached.

FITC-Albumin Loading Within the Hydrogels

A solution of FITC-albumin (1 mg/mL) was obtained by dissolving the protein in PBS solution (pH 7.4). Then, poly[(L-cysteine₅)₄-(StarPEG_{10k})] and poly[(L-cysteine₁₀)₄-(StarPEG_{10k})] were weighed and independently soaked in FITC-albumin solutions for 48 hours at room temperature, in the dark. The saturated hydrogels were then recovered and rinsed free of any unbound FITC-albumin using an excess of PBS solution and stored for further use. The supernatants obtained from the rinsing cycles were retained and analysed for absorbance in order to ascertain the concentration of protein encapsulated in each hydrogel.

Fluorescence Microscopy

Xerogels prepared by lyophilisation of the hydrogels obtained from poly[(L-cysteine₅)₄-*b*-(StarPEG_{10k})] and poly[(L-cysteine₁₀)₄-*b*-(StarPEG_{10k})] were independently soaked in FITC-albumin solutions (1 mg/mL) at room temperature, for 48 hours in the dark. The hydrogels obtained were then mounted on microscope glass-slides.

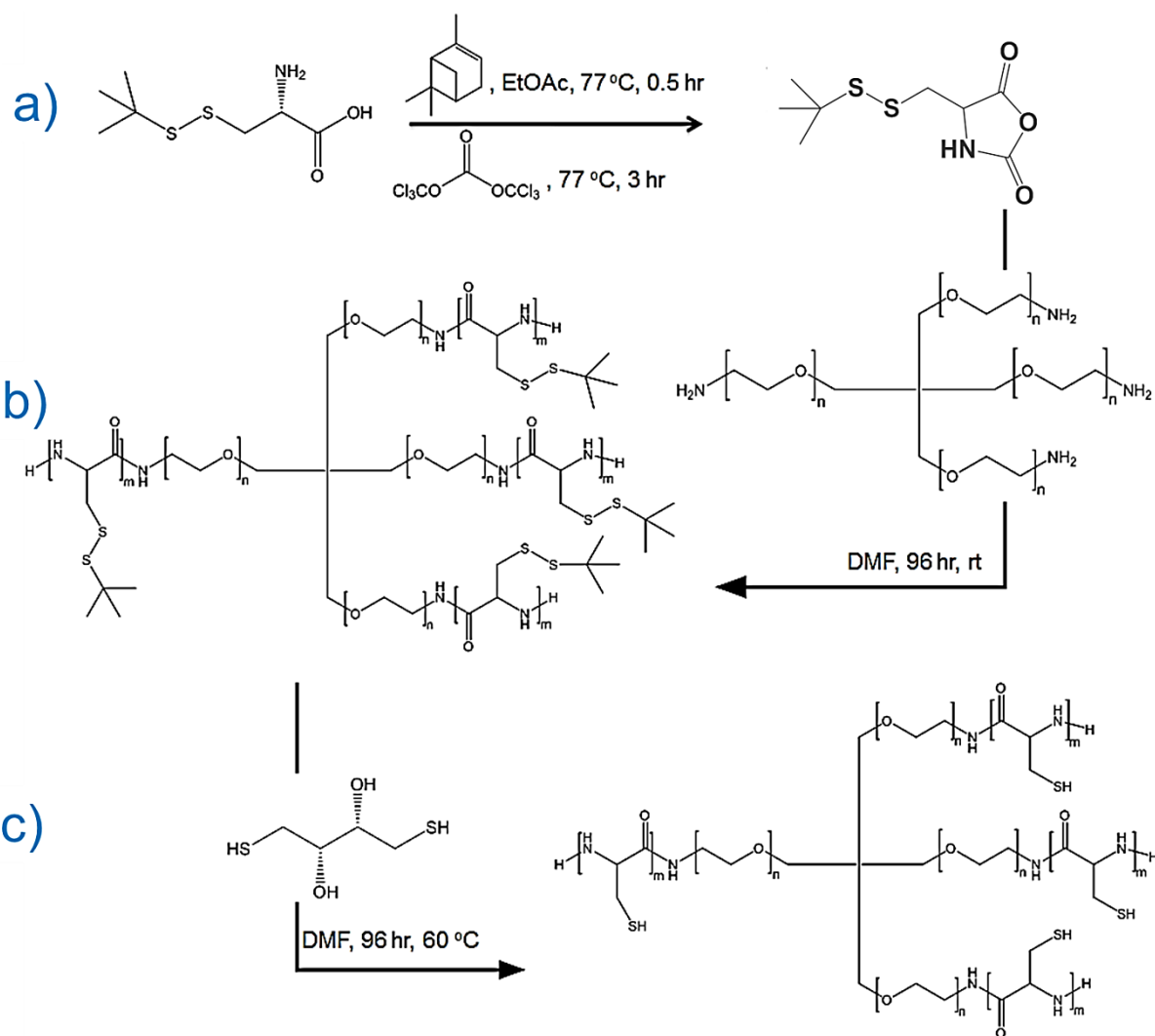
Glutathione-Mediated *In Vitro* Degradation of Hydrogels

Hydrogel degradation was monitored by tracking the release of the encapsulated protein payload. The FITC-Albumin loaded hydrogels were stored in glass vials that contained PBS

solution only (10 mL, pH 7.4) and L-glutathione in PBS solution (5 mM , 10 mL, pH 7.4). The vials were masked with aluminium foil and incubated in an oven maintained at 37 °C. At selected intervals, aliquots (70 µL) were obtained from each vial and analysed by UV-vis spectroscopy. The analysed samples were returned immediately to their parent vials after each analysis. The protein released at each time interval was quantified from the previously obtained linear calibration graph.

Results and Discussion

The NCA of *S-tert*-Butylmercapto-L-cysteine (STBM-L-cysteine NCA) was obtained in good purity using an established protocol (Scheme 1a) [25]. Then, a four-arm, amine-terminated poly(ethylene glycol) (starPEG, Mw: 10,000 Da) was used to initiate the ring opening polymerisation of STBM-L-cysteine NCA in monomer feed ratios of 5, 10 and 20 monomer units per starPEG arm (Scheme 1b) [26]. NCA ROP was performed in anhydrous DMF in order to enable the dissolution of both the macroinitiator, NCA monomer and the resultant polymer. The feasibility of the starPEG-mediated ROP of STBM-L-cysteine NCA was confirmed by ¹H NMR spectroscopy (Figure 1b) and FTIR spectroscopy (Figure 2). Comparison between the ¹H NMR integral values corresponding to the STBM protons (1.46 - 1.81 ppm) and the PEG star polymer initiator protons (3.25 - 4.50 ppm) allowed for the composition of the polymers to be determined (Table 1). The polymerisations to produce the polymers stated in entries **1** and **2** went to completion within the allocated reaction period. The polymerisation detailed in entry **3** did not go to completion due to the increased monomer concentration, and was terminated after 96 hours immediately prior to the reaction mixture becoming turbid; an occurrence that was observed in an independent reaction.



Scheme 1. The route towards the generation of thiol-ene cross-linkable macromolecules: the synthesis of STBM-L-cysteine NCA (a), starPEG amine-mediated NCA ROP to generate poly[(STBM-L-cysteine)_n]₄-*b*-(StarPEG_{10k}) macromolecules (b) and dithiothreitol-mediated reductive removal of STBM groups to generate macromolecules that possess pendant thiol side groups (c).

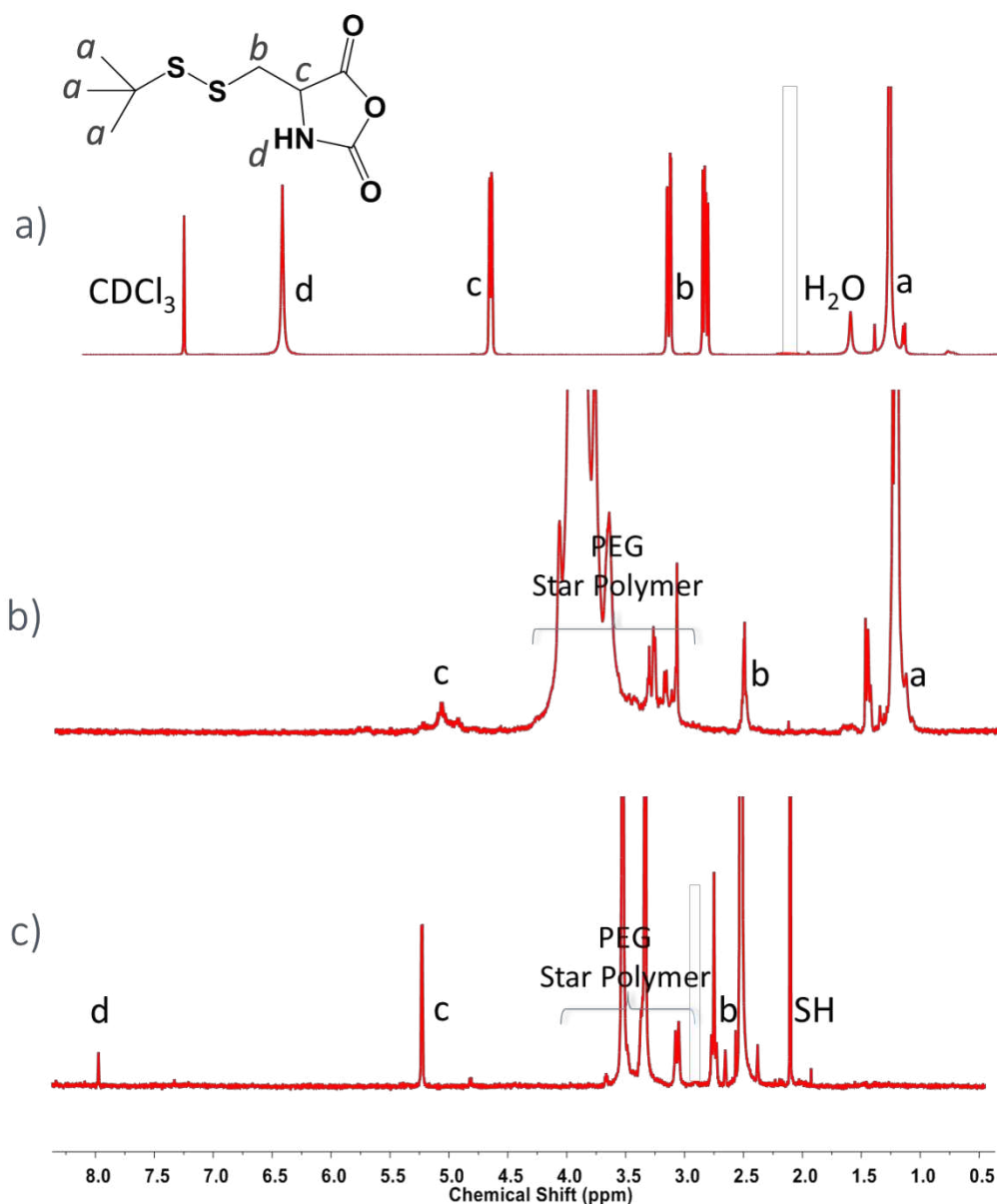


Figure 1. ^1H NMR spectrum of STBM-L-Cysteine NCA (a), representative ^1H NMR spectra in TFA-d for poly[(STBM-L-cysteine) $_n$]- b -(StarPEG $_{10k}$)] macromolecules before removal of STBM protecting groups (b) and after deprotection to remove STBM protecting groups (c).

Infrared spectroscopy (Figure 2) revealed the disappearance of the anhydride stretch (1806 cm^{-1}) of the NCA monomer and the subsequent emergence of the amide stretch after NCA ROP for 96 hours. The emergence of the ether signal ($ca\ 1200 - 1012\text{ cm}^{-1}$) on the infrared spectrum of the hybrid macromolecules, due to the presence of PEG, also confirmed the successful grafting of peptide oligomers from the PEG star polymer initiator. The formation of copolymers was confirmed further by thermal analyses (Figures S2 and S3). The DSC

thermograms of the STBM-protected macromolecules (Figure S2b) reveals the emergence of an endotherm trough (i) at 262-310 °C that is absent on the DSC thermogram of the PEG star polymer macroinitiator (Figure S2a). This endotherm is attributed to the energy required to combust the carbon content which is contributed mostly by the STBM protecting groups. This endotherm was confirmed further by TGA as a weight-loss shoulder that is attributable to combustion (Figure S3iii). As expected, this shoulder is absent from the TGA thermogram of the PEG star polymer macroinitiator (Figure S3v). Successful grafting of the poly(amino acid) was also demonstrated by the presence of the endotherm trough for the melting of the PEG star polymer macroinitiator at 50 °C that is present in the thermograms of the poly(amino acid)-grafted macromolecules. The copolymers produced possessed a monomodal molecular weight distribution, as determined by APC and represented by the chromatogram corresponding to poly[(STBM-L-cysteine₁₀)₄-*b*-(StarPEG_{10k})] (Figure S4).

Table 1. Composition of the copolymers obtained from the NCA ROP.

Entry	Theoretical Macromolecule	Structure as determined by ¹H NMR
1	Poly[(STBM-L-cysteine ₅) ₄ - <i>b</i> -(StarPEG _{10k})]	Poly[(STBM-L-cysteine ₅) ₄ - <i>b</i> -(StarPEG _{10k})]
2	Poly[(STBM-L-cysteine ₁₀) ₄ - <i>b</i> -(StarPEG _{10k})]	Poly[(STBM-L-cysteine ₁₀) ₄ - <i>b</i> -(StarPEG _{10k})]
3	Poly[(STBM-L-cysteine ₂₀) ₄ - <i>b</i> -(StarPEG _{10k})]	Poly[(STBM-L-cysteine ₁₆) ₄ - <i>b</i> -(StarPEG _{10k})]

A standard deprotection procedure was then adopted for the elimination of STBM groups by DTT-mediated reduction of the disulfide linkages to generate free thiol groups (Scheme 1c) [10]. ¹H NMR spectroscopy spectra of the deprotected macromolecules (Figure 1c) revealed

the complete disappearance of STBM ^1H NMR signals (1.26 - 1.71 ppm) and the emergence of a peak that is characteristic of alkyl thiol protons (2.15 ppm).

DSC and TGA analyses of the deprotected macromolecules further confirmed the removal of STBM groups by revealing the disappearance of the endotherm trough (Figure S2c) and decrease in weight-loss shoulder (Figure S3iv) that were observed prior to carrying out the deprotection (Figure S2b and Figure S3 iii), respectively.

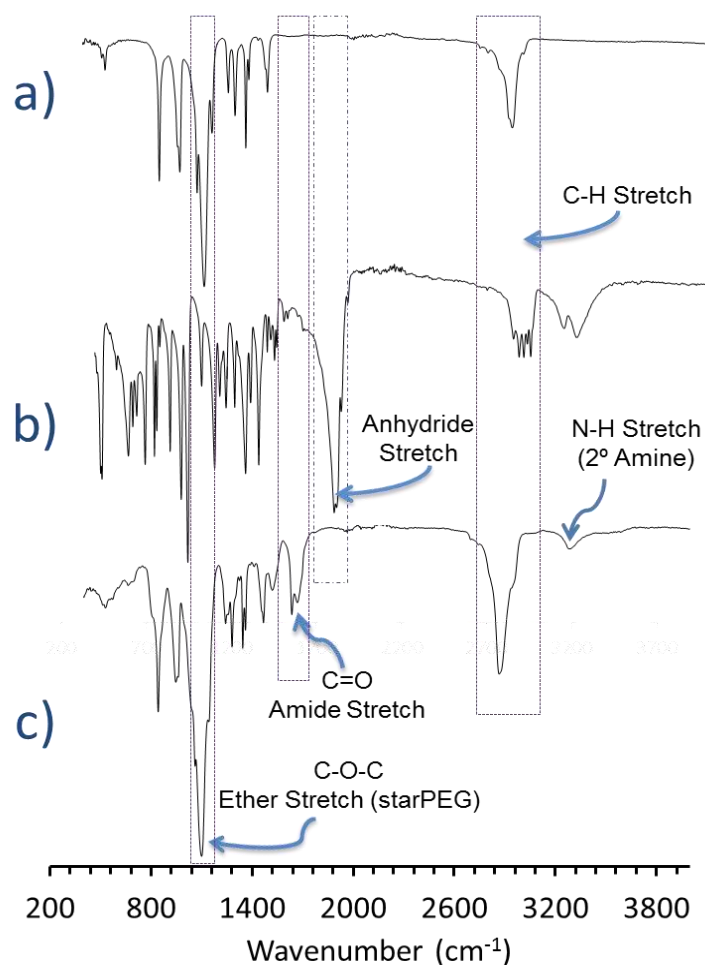


Figure 2. FTIR spectra of PEG star polymer macroinitiator (a), STBM-L-Cysteine NCA (b) and the resultant hybrid macromolecule obtained from the starPEG-initiated ROP of STBM-L-Cysteine NCA (c).

It was anticipated that poly((STBM-L-cysteine)-*b*-(StarPEG_{10k})) may self-assemble in aqueous media to form discrete particles due to its inherent amphiphilicity. Monodisperse particles were formed, the size of which were observed to vary inversely with the length of the

poly(amino acid) block (Figure 3). For example, poly((STBM-L-cysteine₁₆)₄-*b*-(StarPEG_{10k})) aggregated into particles with an average size of 138.8 nm, poly((STBM-L-cysteine₁₀)₄-*b*-(StarPEG_{10k})) aggregated into particles with an average size of 274.7 nm and poly((STBM-L-cysteine₅)₄-*b*-(StarPEG_{10k})) aggregated into particles with an average size of 368.8 nm.

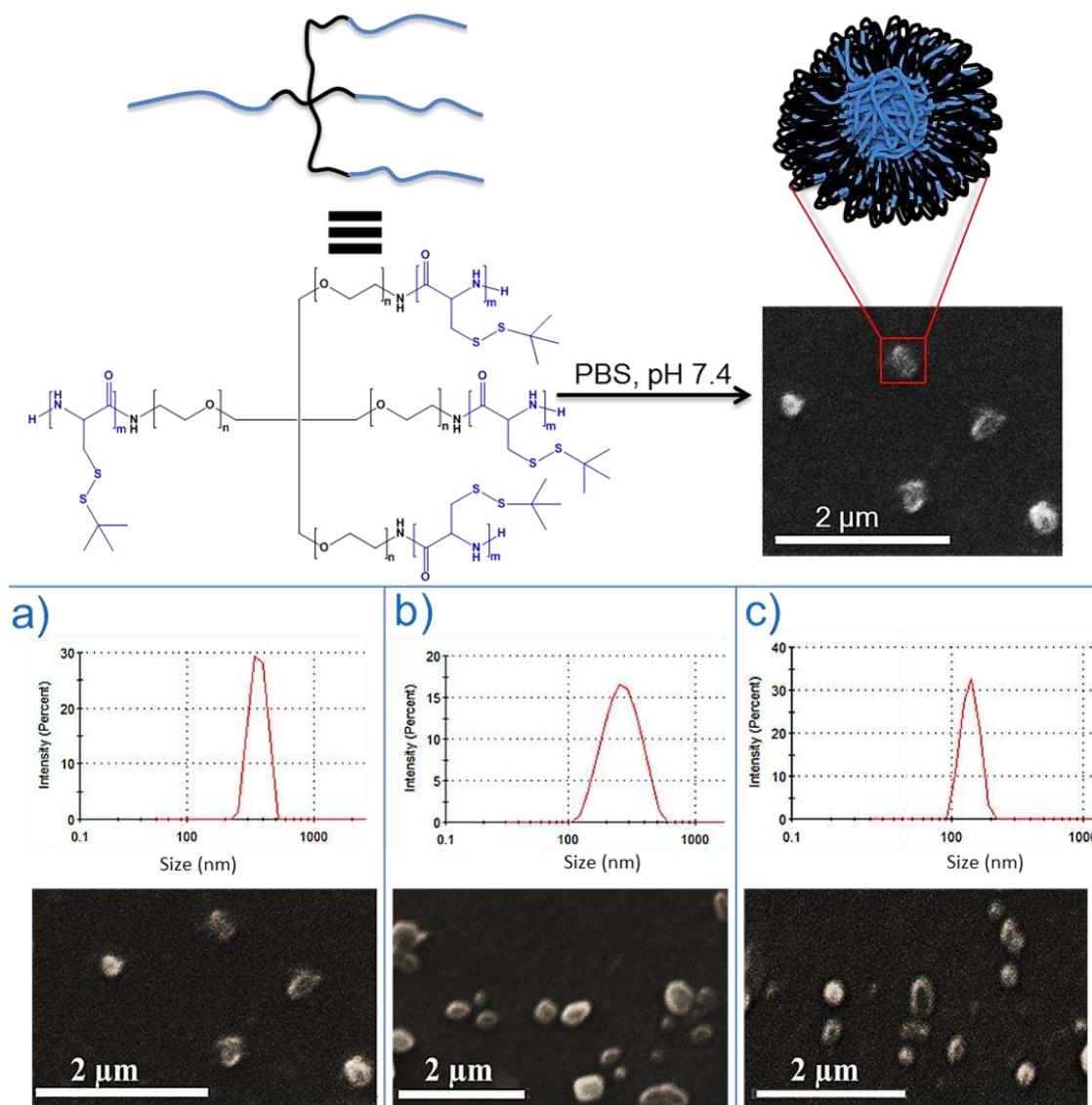


Figure 3. STBM-protected macromolecules self-organise in aqueous medium into spherical particles (*top*). DLS traces and SEM micrographs obtained from the self-assembly of (a) poly[(STBM-L-cysteine₅)₄-*b*-(StarPEG_{10k})], (b) poly[(STBM-L-cysteine₁₀)₄-*b*-(StarPEG_{10k})] and (c) poly[(STBM-L-cysteine₁₆)₄-*b*-(StarPEG_{10k})] macromolecules in aqueous medium.

A literature-reported procedure was then adopted to crosslink the deprotected macromolecules, forming disulfide linkages between adjacent polymer chains (Figure 4) [27].

Due to the insolubility of the crosslinked networks formed, solution-based forms of analyses were impossible. DSC analysis of the crosslinked networks revealed the emergence of an endotherm trough (ii) at 220-255 °C (Figure S2d), which was absent prior to crosslinking (Figure S2c). This endotherm is attributed to the thermal energy that is required to cleave the disulfide crosslinks formed [28].

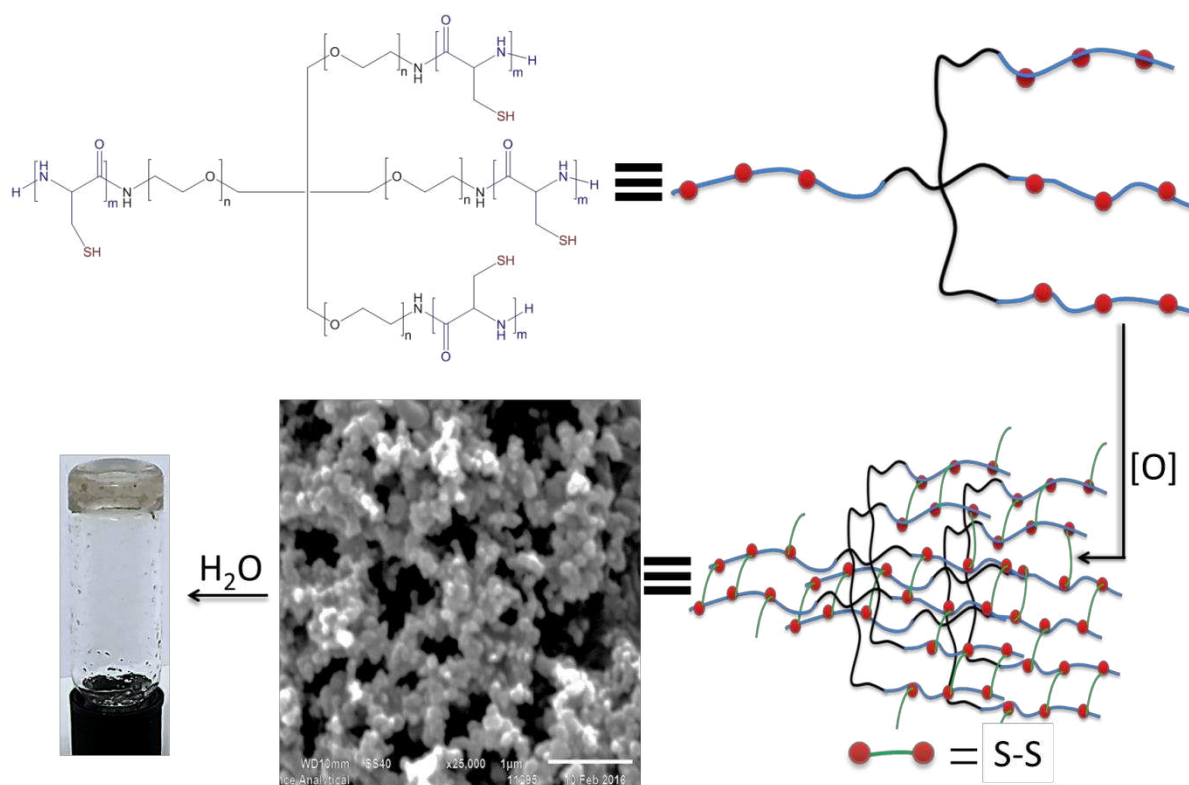


Figure 4. Graphical illustration of the generation of disulfide crosslinked chemical hydrogels.

The morphology of polymer hydrogels is paramount for their successful application as biomaterials. For example, in tissue engineering, the success of cell-proliferation on the polymeric scaffolds is reliant upon the perfusion of nutrients to cells that are able to migrate throughout the polymer network [29,30]. In addition, a porous structure within drug delivery vehicles is advantageous to enable the loading of sufficiently high concentrations of therapeutic agents within the carrier. SEM analysis of the crosslinked polymer xerogels revealed that they possess a microstructure that is characterised by an interconnected porous 3D network (Figure 5a, b).

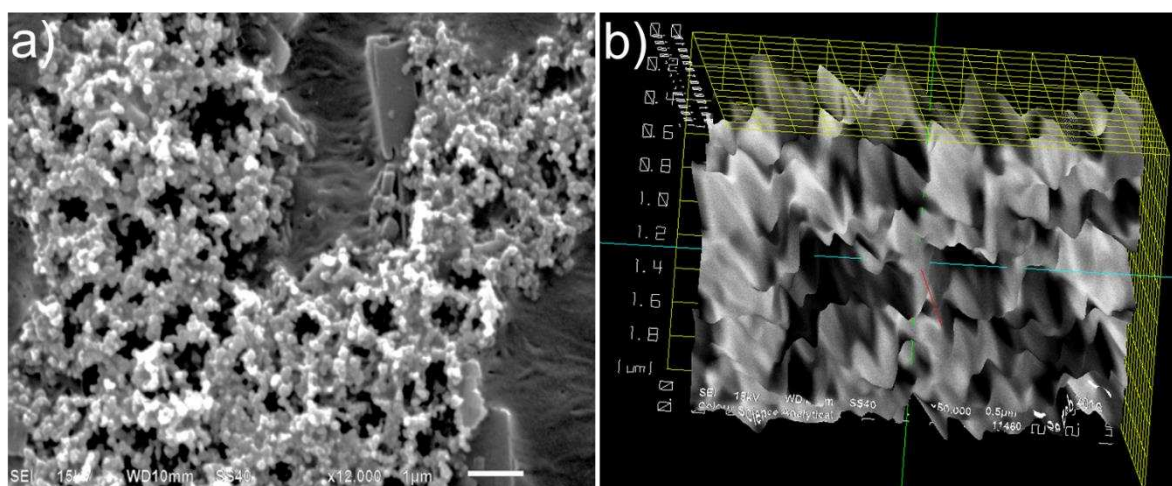


Figure 5. a) SEM micrographs of a poly((L-cysteine₁₀)₄-b-(starPEG_{10k})) chemical hydrogel and b) A 3D micrograph of the hydrogel further reveals the presence of the pores (seen as alternating ‘hills’ and ‘valleys’) within the microstructure.

The pores that exist within the hydrogels’ microstructure are evident in the 3D microphotograph as alternating ‘hills’ and ‘valleys’ (Figure 5b).

The effect of crosslink density on the polymers’ ability to uptake and withhold aqueous medium was investigated by monitoring PBS solution uptake. The uptake varied inversely with the length of the peptide oligomers or the number of cysteine monomer units grafted onto each arm of starPEG (Figure S6). PBS solution uptake peaked (66.1 wt.%) for the hydrogel possessing the shortest peptide oligomers (an average of five cysteine monomer units grafted on each arm of starPEG) but was the least (37.5 wt.%) for the hydrogel possessing the longest peptide block (an average of 16 cysteine monomer units grafted on each arm of starPEG). This could be because of the greater crosslink density of the polymers that contain a greater number of cysteine repeat units, which results in a decrease in porosity and the swelling ability of the hydrogels [31,32].

The poly[(L-cysteine₅)₄-b-(StarPEG_{10k})] and poly[(L-cysteine₁₀)₄-b-(StarPEG_{10k})] hydrogels were then investigated for their ability to withhold the model protein albumin–fluorescein isothiocyanate conjugate (FITC-albumin). The protein-loaded hydrogels were analysed by

fluorescence microscopy to ascertain the extent of FITC-albumin loading and retention following hydrogel washing (Figure S7 a,b). The uniform distribution of green fluorescence within the hydrogels confirms the retention of FITC-labelled protein within the hydrogel networks. UV-vis spectroscopy analysis of the respective supernatants obtained after the washing cycles revealed that 46 wt.% of FITC-albumin was successfully loaded into the poly[(L-cysteine₅)₄-*b*-(StarPEG_{10k})] hydrogel and 49 wt.% was successfully loaded in poly[(L-cysteine₁₀)₄-*b*-(StarPEG_{10k})] hydrogel (0.46 mg and 0.49 mg of FITC-albumin per mg of hydrogel respectively).

An assessment of utilising GSH to activate FITC-albumin release from the hydrogels, by the reduction of the disulfide bridges that maintain the network structure, was then carried out. The release of FITC-albumin from the hydrogels in response to an excessive amount of GSH (See supporting information) was monitored for up to 6 hours. 33.3% of the protein was released from the poly[(L-cysteine₁₀)₄-*b*-(StarPEG_{10k})] hydrogel after 6 hours while 37.1% of the protein was released from the poly[(L-cysteine₅)₄-*b*-(StarPEG_{10k})] hydrogel after 6 hours of incubation at the physiological temperature, respectively (Figure 6). Beyond this time point, hydrogel degradation prevented the extent of release to be determined with accuracy as the isolation of the supernatant from the impaired hydrogel became impossible. On the contrary, less than 2% of the encapsulated FITC-albumin was released when the hydrogels were incubated in PBS solution only. Complete disruption of the crosslinked networks to release the encapsulated cargo was observed when the hydrogels were left for a prolonged period (48 hours) in GSH solutions, as revealed by fluorescence microscopy (Figure S6, c).

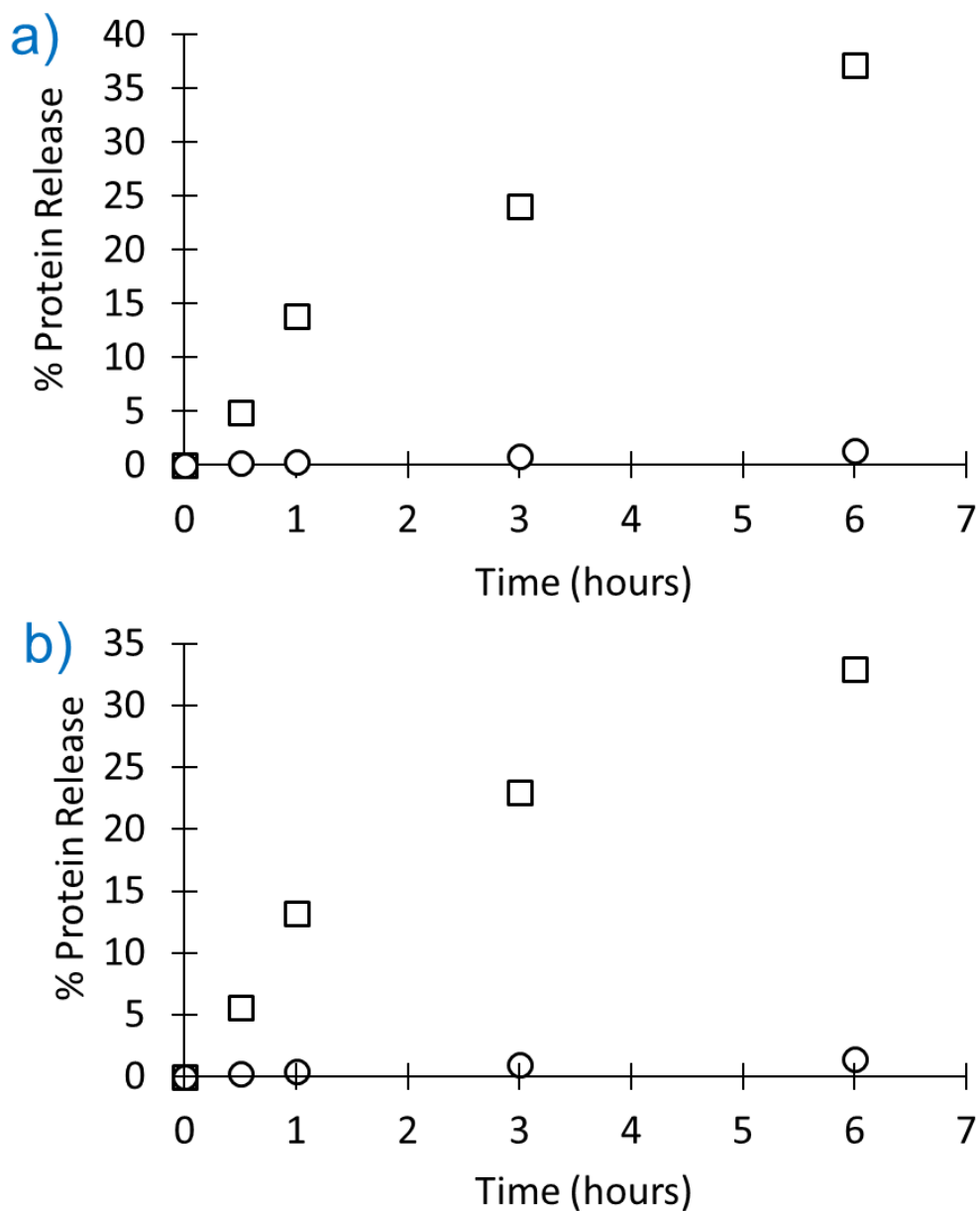


Figure 6. The release of FITC-albumin from a poly[(L-cysteine₅)₄-b-(StarPEG_{10k})] hydrogel (a) and from a poly[(L-cysteine₁₀)₄-b-(StarPEG_{10k})] hydrogel (b) in response to incubation in glutathione (□) and in response to incubation in PBS solution only (○).

These results confirm the suitability of employing the reported materials for the controlled release of protein molecules, with potential application as therapeutic delivery vehicles and/or scaffolds to promote tissue regeneration.

Conclusions

NCA ROP has been employed to furnish StarPEG with terminal cysteine units. Initially, the grafted cysteine units presented tertiary butyl protecting groups, dictating that the modified PEG possesses amphiphilicity and the capability to self-assemble in aqueous solution to form discrete particles. Upon cysteine deprotection, a polymer capable of undergoing chemical crosslinking through the formation of disulfide bridges was isolated. Covalently crosslinked polymer hydrogels were consequently formed that were capable of entrapping FITC-albumin, prior to its release upon disulfide reduction and hydrogel disassembly, mediated by glutathione. The hydrogels reported have particular potential to be utilised for the delivery of (bio)macromolecules at reductive sites, and may further be used as scaffolds for tissue regeneration that aid cell growth and proliferation through the release of protein growth factors.

Acknowledgements

The authors wish to thank the Beit Trust for providing financial support to the research detailed in this paper.

References

- [1] Y. Shen, X. Fu, W. Fu, Zhibo Li, Biodegradable stimuli-responsive polypeptide materials prepared by ring opening polymerization, *Chem. Soc. Rev.*, 44 (2015), pp. 612-622.
- [2] S. Zhang, Z. Li, Stimuli-responsive polypeptide materials prepared by ring-opening polymerization of α -amino acid N-carboxyanhydrides, *J. of Poly. Sci. B: Poly. Phys.* 51(2013), pp.546-555.
- [3] R. Cheng, F. Meng, C. Deng, H.-A. Klok, Z. Zhong, Dual and multi-stimuli responsive polymeric nanoparticles for programmed site-specific drug delivery, *Biomaterials*, 34(2013), pp.3647-3657.
- [4] J. Nicolas, S. Mura, D. Brambilla, N. Mackiewicz, P. Couvreur, Design, functionalization strategies and biomedical applications of targeted biodegradable/biocompatible polymer-based nanocarriers for drug delivery, *Chem. Soc. Rev.*, 42 (2013), pp. 1147-1235.
- [5] H. Wei, R.-X. Zhuo, X.-Z. Zhang, Design and development of polymeric micelles with cleavable links for intracellular drug delivery, *Progress in Poly. Sci.*, 38(2013), pp.503-535.
- [6] R. Langer, J. Vacanti, Advances in tissue engineering, *Journal of Pediatric Surgery*, 51 (2016), pp. 8–12.

- [7] F. Khan, M. Tanaka, S.R. Ahmad, Fabrication of polymeric biomaterials: a strategy for tissue engineering and medical devices, *J. of Materials Chem. B.*, 3(2015), pp.8224-8249.
- [8] H. Cui, Y. Liu, Y. Cheng, Z. Zhang, P. Zhang, X. Chen, Y. Wei, In vitro study of electroactive tetraaniline-containing thermosensitive hydrogels for cardiac tissue engineering. *Biomacromolecules*, 15(2014), pp.1115-1123.
- [9] Y. Pei, O. R. Sugita, J. Y. Quek, P. J. Roth, A. B. Lowe, pH-, thermo- and electrolyte-responsive polymer gels derived from a well-defined, RAFT-synthesized, poly(2-vinyl-4,4-dimethylazlactone) homopolymer via one-pot post-polymerization modification, *European Polymer Journal*, 62 (2015), pp. 204–213.
- [10] S. V. Lale, A. Kumar, F. Naz, A. C. Bharti, V. Koul, Multifunctional ATRP based pH responsive polymeric nanoparticles for improved doxorubicin chemotherapy in breast cancer by proton sponge effect/endo-lysosomal escape, *Polym. Chem.*, 6 (2015), pp. 2115-2132
- [11] L. Liu, L. Fu, T. Jing, Z. Ruan, L. Yan, pH-triggered polypeptides nanoparticles for efficient BODIPY imaging-guided near infrared photodynamic therapy, *ACS App. Mater. & Interfaces*, 8(2016), pp.8980-8990.
- [12] M. Khuphe, B. Mukonoweshuro, A. Kazlauciusas, P.D. Thornton, A vegetable oil-based organogel for use in pH-mediated drug delivery, *Soft Matter*, 11(2015), pp.9160-9167.
- [13] M. Khuphe, A. Kazlauciusas, M. Huscroft, P. D. Thornton, The formation of biodegradable micelles from a therapeutic initiator for enzyme-mediated drug delivery, *Chem. Commun.*, 51 (2015), pp. 1520-1523.
- [14] F. Meng, W.E. Hennink, Z. Zhong, Reduction-sensitive polymers and bioconjugates for biomedical applications, *Biomaterials*, 30 (2009), pp. 2180-2198.
- [15] H. Zhang, X. Kong, Y. Tang, W. Lin, Hydrogen sulfide triggered charge-reversal micelles for cancer-targeted drug delivery and imaging. *ACS App. Mater. & Interfaces*. 2016.
- [16] Q. Zhou, L. Xu, F. Liu, W. Zhang, Construction of reduction-responsive photosensitizers based on amphiphilic block copolymers and their application for photodynamic therapy, *Polymer*, 97(2016), pp.323-334.
- [17] B. Arunachalam, U. T. Phan, H. J. Geuze, P. Cresswell, Enzymatic reduction of disulfide bonds in lysosomes: Characterization of a Gamma-interferon-inducible lysosomal thiol reductase (GILT), *Proc Natl Acad Sci U S A*, 97 (2000), pp. 745-750.
- [18] C. Wu, C. Belenda, J.-C. Leroux, M. A. Gauthier, Interplay of chemical microenvironment and redox environment on thiol–disulfide exchange kinetics. *Chem.–Eur. J.* 17 (2011), pp. 10064–10070.
- [19] T. Vermonden, R. Censi, W. E. Hennink, Hydrogels for protein delivery, *Chem. Rev.* 112 (2012), pp. 2853–2888.
- [20] D. Seliktar, Designing cell-compatible hydrogels for biomedical applications, *Science*, 336 (2012), pp. 1124-1128.
- [21] P. D. Thornton, A. Heise, Bio-functionalisation to enzymatically control the solution properties of a self-supporting polymeric material, *Chem. Commun.* 47 (2011), pp. 3108-3110.
- [22] T. Hayashi, P. D. Thornton, The Synthesis and Characterisation of Thiol-Bearing C. I. Disperse Red 1. *Dyes Pigments*, 121 (2015), pp. 235-237; T Hayashi, A. Kazlauciusas, P. D.

Thornton, Dye conjugation to linseed oil by highly-effective thiol-ene coupling and subsequent esterification reactions, *Dyes Pigments*, 123 (2015), pp. 304-316.

[23] S-Y. Lee, S. Kim, J. Y. Tyler, K. Park, J-X. Cheng, Blood-stable, tumor-adaptable disulfide bonded mPEG-(Cys)4-PDLLA micelles for chemotherapy, *Biomaterials*, 34 (2013), pp. 552-561.

[24] P. D. Thornton, R. Brannigan, J. Podporska, B. Quilty, A. Heise, The generation of hydrophilic polypeptide-siloxane conjugates via N-carboxyanhydride polymerisation, *J. Mater. Sci: Mater. Med.* 23(2012) pp. 37-45.

[25] B.J. Sparks, J.G. Ray, D.A. Savin, C.M. Stafford, D.L. Patton, Synthesis of thiol-clickable and block copolypeptide brushes via nickel-mediated surface initiated polymerization of [small alpha]-amino acid N-carboxyanhydrides (NCAs). *Chem. Commun.* 47(2011), pp.6245-6247.

[26] P.D. Thornton, S.M.R. Billah, N.R. Cameron, Enzyme-degradable self-assembled hydrogels from polyalanine-modified poly(ethylene glycol) star polymers. *Macromol. Rapid Commun.* 34(2013), pp.257-262.

[27] G.J.M. Habraken, C.E. Koning, J.P.A. Heuts, A. Heise, Thiol chemistry on well-defined synthetic polypeptides. *Chem. Commun.*, 24(2009), pp.3612-3614.

[28] Y. Dou, B. Zhang, M. He, G. Yin, Y. Cui, I.N. Savina, Keratin/polyvinyl alcohol blend films cross-linked by dialdehyde starch and their potential application for drug release, *Polymers*. 7(2015), pp.580-591.

[29] G. Ahuja, K. Pathak, Porous carriers for controlled/modulated drug delivery. *Indian J. of Pharma. Sci.*, 71(2009), pp.599-607;

[30] S.-E. Lamhamedi-Cherradi, M. Santoro, V. Ramammoorthy, B.A. Menegaz, G. Bartholomeusz, L.R. Iles, H.M. Amin, A.J. Livingston, A.G. Mikos, J.A. Ludwig, 3D tissue-engineered model of ewing sarcoma. *Adv. Drug Deliv. Revs.*, 2014, pp.155-171.

[31] J. Maitra, V.K. Shukla, Cross-linking in hydrogels-a review, *American J. of Poly. Sci.*, 4(2014), pp.25-31; K.Y. Lee, J.A. Rowley, P. Eiselt, E.M. Moy, K.H. Bouhadir, D.J. Mooney, Controlling mechanical and swelling properties of alginate hydrogels independently by cross-linker type and cross-linking density, *Macromolecules*, 33(2000), pp.4291-4294.

[32] H.V. Chavda, C.N. Patel, Effect of crosslinker concentration on characteristics of superporous hydrogel, *Int. J. of Pharma. Investigation*, 1(2011), pp.17-21.

Graphical Abstract

